The potential of major ion chemistry to assess groundwater vulnerability of a regional aquifer in southern Quebec (Canada)

G. Meyzonnat [1], M. Larocque [1*], F. Barbecot [1], D.L. Pinti[1], S. Gagné [1]

[1]*Département des sciences de la Terre et de l'atmosphère and GEOTOP, Université du Québec à Montréal, C.P. 8888, Succursale Centre-Ville, Montreal (Québec), Canada, H3C 3P8*

**Corresponding author: larocque.marie@uqam.ca;(514)-987-3000 # 1515*

Abstract

Groundwater vulnerability mapping provides useful but limited information for developing protection plans of the resource. Classical vulnerability ranking methods often do not take into account complex hydro-stratigraphy and never consider groundwater flow dynamics. The objective of this work was to test the potential of major ion chemistry to assess regional scale intrinsic groundwater vulnerability. Because it reflects water-sediment and water-rock interactions, the new vulnerability index reflects both infiltration processes and groundwater hydrodynamics. The method was applied on a regional fractured bedrock aquifer located in the Becancour region of southern Quebec (Canada). In this region, hydrogeochemistry shows that freshly recharged groundwater evolves from (Ca,Mg)-HCO_3 and Ca-SO_4 to Na-HCO_3 type with gradually increasing confinement conditions in the fractured aquifer, and tends to Na-Cl type locally by mixing with trapped marine pore-water. The new method identified recharge areas as those of highest vulnerability and gradually decreasing vulnerability as confinement of the aquifer increased. It also highlights local discontinuities in confinement that differ from the regional pattern. Results showed a good correlation between groundwater vulnerability estimated with the new method and nitrate occurrence in groundwater. Eighty-two percent of all samples presenting detectable nitrate concentrations were characterized by a Hydrogeochemical Vulnerability Index greater than 9 (maximum is 10). The ability of the new vulnerability method to identify areas vulnerable to detectable nitrate concentrations was much higher than that deriving from the DRASTIC method. This work confirms that major ions chemistry contains significant information about groundwater vulnerability and could be used to improve groundwater resource management.

Keywords
Groundwater, vulnerability, hydrogeochemistry, fractured bedrock aquifer, Quebec (Canada)

Introduction

In the last decades, worldwide increases in groundwater contamination (UNEP 2003) have brought attention to the concept of groundwater vulnerability and led to the development of specific mapping techniques. Groundwater vulnerability is generally defined as the capacity of a hydrogeological system to transfer a contaminant from the land surface to the saturated zone. This concept is continuously evolving and several definitions have been proposed. For example, intrinsic vulnerability (Vrba and Zoporozec 1994) and intrinsic sensitivity (EPA 1993) usually refer to groundwater vulnerability due to the hydrogeological context independently of land use or any information about the spatial distribution of potential sources of contamination. The specific vulnerability (Andrade and Stigter 2009) integrates contaminant-specific parameters, such as half-life or sorption coefficient to soil organic matter when assessing groundwater vulnerability to pesticides. In reference to the source-pathway-target concept, the contaminant pathway for "aquifer vulnerability" is the vertical path from the ground surface to the water table. When considering "well vulnerability" (Frind et al. 2006) the contaminant pathway is the flow path from an upgradient source at ground surface to a given well.

Many methods are available to estimate intrinsic groundwater vulnerability. Ranking or index-based aquifer vulnerability methods such as DRASTIC (Aller et al. 1987), AQUIPRO (Chowdhury 2003) or LHT (Mansoor 2014) might be the easiest methods to implement using available physical data. These methods are currently widely used in water management as land-use planning tools and often reported in the scientific literature (see Saidi 2010; Tilahun 2010; Chen 2013; or Mansoor 2014 for recent applications of the DRASTIC index). However, index methods raise criticism because they often fail to predict the occurrence of contaminants in groundwater (Mehnert et al. 2005; Stigter et al. 2008). One reason could be because indexed aquifer vulnerability methods do not take into account groundwater flow dynamics, which may control the lateral migration of contaminants from the land surface to the aquifer (Kozuskanich 2014). The scientific literature holds many examples of modification and adaptation of index methods intended to increase their reliability in specific contexts or to increase their efficiency to correlate with contaminant occurrence (Bojórquez-Tapia et al. 2009; Zhou 2012; Chen 2013).

The estimation of travelling time through the vadose zone could serve as an indicator of aquifer vulnerability (Van Stempvoort 1992) but requires data extracted from geological 3D models which are often unavailable. At the opposite end, numerical models of solute transport through vadose and saturated zones (Yu 2014) aim to represent all relevant processes influencing well vulnerability. These methods integrate flow dynamics and are very useful for assessing the risk of anthropogenic pollution to potable water supplies (Frind et al. 2006), but have large data requirements (Nobre 2007).

Another way to integrate groundwater flow processes is to consider groundwater geochemistry. Major ions water chemistry (Ca, Mg, K, Na, Cl, HCO_3 and SO_4) is the product of water-soil and water-rock interactions (e.g., Barbecot et al. 2000; Sanexa 2001). Because they depend on flow paths and on groundwater residence times, major ion facies are often used to determine the natural baseline composition of groundwater (Edmunds et al. 2003) or to distinguish between contrasted hydrogeological contexts (Cloutier et al. 2008). Hydrogeochemistry can also be useful to assess groundwater quality through statistical regression of chemical trends (Stigter et al. 2008). Multivariate analyses of geochemical data have been used to build groundwater quality indices, and typically include solutes from natural and/or anthropogenic origin (Saeedi et al. 1998).

Hydrogeochemistry closely reflects input from recharge areas, as well as confinement conditions and groundwater travel times. It is therefore a proxy for groundwater vulnerability. Recharge areas represent direct links between the surface and the saturated zone, characterized by a distinct water signature. Aquifer confinement usually implies a longer rock-water contact time. And, as travel time increases, the possibility of degradation (e.g., denitrification; see McMahon et al. 2008), cation adsorption (e.g., on clay matrix; Andrade and Stigter 2009) and dilution within the regional aquifer flow also increase. Although groundwater quality indices are useful to distinguish more or less vulnerable areas, they mostly portray regional quality of groundwater (Sorichetta et al. 2013). Mendizabal and Stuyfzand (2011) have explicitly defined an intrinsic well vulnerability index by integrating several hydrogeochemical parameters (i.e., pH, redox level, alkalinity and groundwater age as pre- or post-tritium bomb peak). However, this method does not focus on the basic evolution of the major ion composition of groundwater within various hydrogeological contexts.

Hydrogeochemistry has the potential to represent complex influential patterns regarding well vulnerability which otherwise could be extremely difficult to determine at the regional scale with physical approaches. The objective of this work was to test the potential of major ion chemistry to

assess regional scale intrinsic groundwater vulnerability. A new vulnerability index based on the groundwater major ions facies is applied to a regional-scale fractured bedrock aquifer located in the Becancour River watershed in southern Quebec (Canada). The vulnerability index is compared to a regional groundwater vulnerability map drawn with the DRASTIC index and the capacity of both methods to identified measured groundwater nitrate concentrations is assessed.

Geological and hydrogeological setting

The study area is located in southwestern Quebec (Canada) and it covers 2,920 km^2 in the northern portion of the Becancour River watershed (Fig. 1). The northwestern part corresponds to the St. Lawrence Lowlands with flat topography and elevations below 150 masl. The southeastern part is located in the Appalachian Mountains and is marked by an irregular topography reaching maximum elevations of 500 masl. The two regions correspond geologically to the St. Lawrence Platform and the Appalachian Mountains (Fig. 2; Globensky 1993). The Ordovician geological units of the St. Lawrence Platform outcropping in the study area are the Nicolet Fm. and the Saint-Sabine les Fonds Fm. which consist of thick successions of mudstones with subordinate alternating sandstone and siltstone. The outcropping terrains in the Appalachian Mountains correspond to imbricated thrust sheets produced during the Taconian orogeny: green and red shales of the Sillery Group; bedded black weathered shaly matrix containing chaotic blocks of cherts; sandstone of the Etchemin River; and dolomitic schists of the West Sutton Formation.

Unconsolidated Quaternary sediments, derived from multiple glaciation-deglaciation cycles, unconformly cover the Cambrian-Ordovician sequence of the St. Lawrence Lowlands (Lamothe 1989). Within the Appalachian Mountains, Quaternary deposits generally consist of relatively thin layers of till deposited directly on the bedrock (Fig. 2). A more complex Quaternary stratigraphy is found in the St. Lawrence Lowlands. A nearly continuous till sheet (Gentilly till) covers most of the area between the overlain discontinuous marine and lacustrine silt (Lampsilis Lake silts) and clay units of the Champlain Sea (9.8 to 11.2 ka) and the underlain discontinuous patches of sands deposited during marine regressions (Vieilles Forges and Lotbinière sands; Lamothe 1989) with thermo-luminescence measured ages of 44-50 ka (Godbout et al. 2013). Granular deposits thick enough to form aquifers are present downstream of the basin, but have limited regional extents.

Marine clay deposits are found below 120 masl where they create increasingly confining conditions for the bedrock aquifer towards the lower portion of the basin (see Fig. 3).

The regional aquifer is located in the fractured bedrock of the St. Lawrence Platform. This aquifer is mainly unconfined in the Appalachian Mountains and in the Appalachian Piedmont, progressively becoming semi-confined, north-westerly. In a 10 km wide zone bordering the St. Lawrence River, the aquifer is confined by thick marine clays of the Champlain Sea that allow limited recharge (Larocque et al. 2013). The bedrock aquifer within the study area has relatively low hydraulic conductivity (~10^{-9} to 10^{-7} m/s). Wells in the fractured bedrock aquifers yield enough water to supply single-family dwellings and small municipalities (~500 to 5,000 habitants). Higher-yield aquifers (~10^{-3} to 10^{-4} m^2/s) are found in coarse-grained surficial sediments, such as the Quaternary glaciofluvial or fluvial sediments. These are often separated from the fractured bedrock aquifer by a basal till unit (Becancour till; Lamothe 1989), which acts as an aquitard. Regional groundwater flow is SE-NW and usually follows the topography, with recharge occurring mainly in the Appalachian Mountains and discharge in the main tributaries of the St. Lawrence River. Local recharge areas are also found in the St. Lawrence Lowlands, particularly in the absence of Champlain Sea clays, along a band located just northwest of the Appalachian Piedmont. Larocque et al. (2013) estimated the average regional recharge to be 159 mm/yr.

Land use is mainly forestry (48 %) and agricultural (40 %), with the significant presence of wetlands (8 %) and few urban areas (4 %). Cereals and most intensive crops are found mainly along the St. Lawrence and Becancour rivers, while the Appalachian valleys are associated with pastures and dairy farms (see Larocque et al. 2013 for more information on land use). The average annual temperature is 4.5°C, and the total precipitation is 1,100 mm/year, with 25% falling as snow between November and March (Environment Canada 2012).

Analytical methods and groundwater sampling

A total of 84 open borehole bedrock wells (79 domestic or municipality wells and five drilled observation wells) were sampled in July and August 2010. Well depths range from 8 to 144 m, with a median depth of 38 m and only three wells deeper than 100 m (Table 1). This indicates that the upper bedrock is the most productive zone and is probably the bedrock through which most of the groundwater flows. In municipal wells, groundwater was collected directly at the wellhead. For

domestic wells, groundwater was collected at the closest water faucet, taking precaution to avoid intermediate treatment installations. At each sampling site, purge time was set by monitoring the groundwater chemo-physical parameters (conductivity, pH, Eh, and temperature) using a flow-through cell, until they stabilize. Groundwater was sampled in 250 ml PE bottles and filtered *in situ* using disposable 0.45 µm nitrocellulose filters on 60 ml PE syringes. Samples for cation analyses were acidified with HNO_3. The samples were kept at 4°C until their analysis at the Maxxam Laboratory in Montreal (Quebec, Canada). Major cations (Ca, Mg, Na) were analysed with ICP-MS, major anions (Cl and SO_4) were analyzed by ionic chromatography, alkalinity as $CaCO_3$ was measured by titration method at pH 4.5. Finally, nitrate concentration was measured with the hydrazine reduction method. Details of these analytical methods can be found in CEAEQ (2014).

DRASTIC index computation

The DRASTIC index (Aller et al. 1987) was computed using the usual seven parameters and associated parametric weights and ratings:

$$\text{DRASTIC index} = D\,W_D + R\,W_R + A\,W_A + S\,W_S + T\,W_T + I\,W_I + C\,W_C \quad \text{(eq. 1)}$$

Where D is the depth to the water table, R is recharge, A is the aquifer lithology, S is the soil type, T is the topography, I represents the impact of the vadose zone and C is the hydraulic conductivity. Parameter weights are from Aller et al. (1987), i.e. W_D=5, W_R =4, W_A=3, W_S=2, W_T=1, W_I=5, W_C=3.

The DRASTIC index was computed as suggested by Aller et al. (1987) without any adaptation of the usual method to the geological context or contaminant occurrence in groundwater in order to neutrally apply the method. Depth to groundwater (*D*) was estimated by subtracting piezometric levels from the digital elevation model (MRNF, 2008). Where the bedrock aquifer is confined, *D* was set equal to the bedrock depth below unconsolidated sediments. Recharge (*R*) was determined with a spatially-distributed water balance model with a 500 x 500 m resolution. Regional piezometric surface and spatially distributed recharge to the bedrock were established by Larocque et al. (2013). The bedrock aquifer lithology (*A*) was determined following Globensky (1987; 1993) who reports detailed local stratigraphy of the Cambro-Ordovician St. Lawrence Platform and the

Appalachian Mountains. Soil type (*S*) was obtained from pedologic maps from IRDA (2012) which provides information about soil granulometry and drainage capacity to be classified with the usual DRASTIC ratings. The slope (*T*) was determined using a GIS treatment of a 10 m-cell resolution digital elevation model (MRNF 2008). The impact of the vadose zone (*I*) was determined from detailed Quaternary deposits maps from Godbout et al. (2011) which gives the type of granulometry associated with clay, silts, sands and glacial tills. Parameter (*I*) for the bedrock aquifer was determined from bedrock lithology description of Globensky (1987; 1993). Again, the classification here refers to soils or bedrock type obtained from available maps of the study area and ratings were directly associated to the typical ratings as defined by Aller et al. (1987). The bedrock hydraulic conductivity (*C*) was set to the minimal ranking value of 1 for the entire study area since all field-measured hydraulic conductivities (Larocque et al. 2013) were lower than the threshold for $C = 1$.

Results and discussion

Regional hydrogeochemistry of the study area

Groundwater chemistry types were determined from the Piper diagram (Fig. 4). Fifty-six percent of the samples belong to the Ca,Mg-HCO_3, Ca-HCO_3 and Ca-SO_4 water types, mainly present in the Appalachian region where unconfined conditions prevail (see Fig. 3). Thirty-nine percent of the samples belong to the Na-HCO_3 water type, representing semi-confined conditions in the flat, central part of the study area to captive conditions in the downstream portion. Five percent of the samples belong to the Na-Cl water type located in the lower portion of the aquifer. The Na-Cl water type represents confined conditions and is associated to a mixing with trapped marine pore-water. Charron (1978), Cloutier et al. (2008, 2010), Beaudry (2013) and Benoit et al. (2014) described similar hydrogeochemical facies for other southern Quebec bedrock aquifers.

In the recharge area, groundwater chemistry is first controlled by the dissolution of carbonates present in calcareous Quaternary deposits such as tills (Cloutier et al. 2010) and through the first few meters of the fractured bedrock aquifer (Edmunds et al. 2003) which is here dominated by calcareous shaly and silty deposits of Ordovician age (Globensky 1987). In the study area, groundwater typically evolves from Ca,Mg-HCO_3 water types with low but nearly equal proportions of Na^+ and Cl^- (representing an initial load of Na-Cl from precipitation) and with equal proportions of $Ca^{2+}+Mg^{2+}$ and $HCO_3^-+SO_4^{2-}$ (from the initial congruent dissolution of calcareous, dolomitic materials). Slower and deeper circulation, involving long-term water-rock interactions in

fractured aquifers, generally involves other processes such as incongruent dissolution of carbonates and cation exchange (Edmunds 1987). For most of the samples taken in the Becancour bedrock aquifer, cation exchange ($Ca^{2+} \rightarrow Na^{+}$) appears to be the controlling process (Fig. 5), leading to the relative enrichment of Na^{+} versus Cl^{-} and relative depletion of $Ca^{2+}+Mg^{2+}$ versus $HCO_3^{-}+SO_4^{2-}$ toward the evolution of groundwater to the Na-HCO_3 type (Cloutier et al. 2010). Na^{+} is released in groundwater by cationic exchange on the clay fraction, whereas Ca^{2+} is depleted from groundwater. For samples with lower (Ca+Mg)/(Na+K) ratios, located in captive groundwater flow conditions, a shift (grey circle Fig. 5) in the total cation content probably indicates a mixing with the seawater end-member. In the study area, Na-Cl is released from marine clays or trapped Champlain Sea seawater (Cloutier et al. 2010), and groundwater evolves to Na-Cl type.

Nitrate concentrations are relatively low, with a maximum value of 6.1 mg N-NO_3/L (drinking water limit 10 mg N-NO_3/L; MDDEFP 2013) and not related to the well depth (Table 1). These concentrations are similar to those reported in other studies from southern Quebec (MENV 2004). Eleven wells (12.9%) mainly located in the Appalachian foothills, have concentrations exceeding 1 mg/L N-NO_3 i.e. the anthropogenic background (Dubrovsky et al. 2010). Low nitrate concentrations in the study area could be attributed to the high recharge rates (159 mm/yr, Larocque et al. 2013) which induce significant dilution within the aquifer (Andrade et al., 2009). They could also be due to the interception of nitrate-rich infiltrated water by agricultural drains (Qi et al. 2011), and to denitrification (see further discussion below).

Hydrogeochemical Vulnerability Index

Considering the hydrogeochemical processes occurring in the study area, plotting the relative differences of Na^{+}-Cl^{-} against $(Ca^{2+}+Mg^{2+})$-$(HCO_3^{-}+SO_4^{2-})$ illustrates how groundwater composition evolves from a Ca,Mg-HCO_3 type in the recharge area to a Na-HCO_3 type down-gradient with gradually increasing confinement conditions (R^2=0.97; Fig. 6). A Hydrogeochemical Vulnerability Index (HVI) from 1 to 10 was attributed to each of the water samples from its orthogonal projection on the linear regression. The HVI identifies the highest vulnerability scores for groundwater samples near the recharge area (Ca, Mg-HCO_3, Ca-HCO_3 and Ca-SO_4 types). It gradually decreases with increasing confinement conditions of the bedrock aquifer, thus changing to Na-HCO_3 type and then Na-Cl type. A HVI map was interpolated (inverse distance weighting)

using all the sampled wells (Fig. 7). The highest values of HVI are found in the Appalachian Mountains (HVI above 8) and gradually decrease with the regional groundwater flow, as the Quaternary deposits become thicker and/or more impermeable. Approaching the St. Lawrence River, the least vulnerable areas (HVI between 1 and 5) correspond to the location of thick clay deposits which confine the bedrock aquifer. The HVI generally reflects the bedrock aquifer confinement conditions (see Fig. 3) but also locally highlights the discontinuities in confinement that differ from the regional pattern. For example, the HVI shows probable local recharge areas within dominantly confined conditions (HVI above 8), particularly downstream, in the northeastern part of the basin and in the Appalachian Piedmont.

The HVI can be derived similarly for other hydrogeological contexts where calcareous dissolution from recharge and Ca^{2+}-Na^{+} cation exchange dominate the water chemistry. This is a common pattern regarding the evolution of groundwater geochemistry composition along the flowpaths (Edmunds 2003; Appelo and Postma 2005). The HVI is expected to be particularly suitable in glacial hydro-geomorphological contexts, i.e. with the presence of calcareous materials found in tills, in sedimentary bedrock rich in clay minerals, and under gradual confinement conditions of the fractured aquifer with marine clays. The HVI was tested in other regions of the St. Lawrence Lowlands in southern Quebec, taking advantage of newly available hydrogeochemical datasets from the Nicolet and lower Saint-François watersheds (Larocque et al. 2015) and in the Monteregie region (Carrier et al. 2013). For these regions, the HVI was built using the same ranges of Na-Cl (y-axis) and Ca+Mg-HCO_3-SO_4 (x-axis) than for the current study area. HVI values larger than 9 were found respectively for 83% and 89% of wells with detectable nitrate (above 0.1 mg N-NO_3/L) (results not illustrated). In other geological and climatic contexts, it might be necessary to modify the axes ranges of Fig. 6 to adjust to site-specific conditions.

The HVI provides integrative information on well vulnerability while being relatively inexpensive to implement and easily computed. Similarly to other types of interpolated maps (e.g. maps of hydrogeological contexts interpolated from local drilling data), the uncertainty related to the interpolated surface is directly linked to data point density. For example, because municipal and private wells are rare near the St. Lawrence River (due to high salinity groundwater), the vulnerability map in the lower portion of the study area is more uncertain. In the case of local groundwater contamination, the method may show heterogeneities related to anthropogenic sources

(e.g., Na-Cl pollution from de-icing road salts, surface water infiltration into a poorly maintained well cap) rather than to the natural hydrogeological context.

DRASTIC vulnerability map

The calculated DRASTIC indices range from 33 to 179 (Fig. 8). This scope is comparable with existing DRASTIC maps obtained in similar geomorphological contexts in southern Quebec (Champagne 1990; Murat 2000). In the current study, the DRASTIC index in the Appalachians indicates the simultaneous presence of medium (between 76 and 100) and high (between 126 and 150) aquifer vulnerability areas. Low groundwater levels on topographic ridges counterbalance high recharge rates. Areas where the aquifer vulnerability is very high higher than 150) are characterized by the presence of granular glaciofluvial deposits where the groundwater depth is shallow. These are found in the valley bottom of the Becancour River in the eastern part of the study area. The index is high (between 126 and 150) to very high (higher than 150) in the central part of study area due to high groundwater levels in a flat topographic context, as well as to the presence of regressive and aeolian sand deposits. In this part of the study area, recharge rates can be high but are counterbalanced by the presence of silty deposits and peatlands (between 76 and 100) which lowers parameters *S* (soils) and *I* (impact of the vadose zone). Low aquifer vulnerability areas (between 33 and 75) are located in the lower part of the basin where thick clay deposits are present.

It is not possible to integrate complex sequences of overlying Quaternary deposits when using the DRASTIC index to estimate the vulnerability of a bedrock aquifer. This is due to the fact that it uses only two parameters for the overlying unconsolidated sediments, i.e. one parameter for soil type (*S*) and another parameter for the impact of the vadose zone (*I*). Recharge is usually the main vector for solute transport through the vadose zone, as highlighted in other studies the importance of recharge in aquifer vulnerability estimation (e.g.: Rupert, 2001, Nobre et al. 2007). This is reflected in the index, where four out of seven parameters relate to infiltration and recharge processes (*R*, *S*, *T* and *I*). On the DRASTIC map (Fig. 8), the most extended and vulnerable aquifer zones are found in the Appalachian Piedmont, while hydrogeochemistry suggests that recharge areas are predominantly located in the Appalachian Mountains. High aquifer vulnerability in this area is caused by high *S* and *I* parameters in the presence of sandy soils. However, these regressive and aeolian sands are often superficial deposits covering thick till deposits considered as aquitards.

This underlying till probably offers a good protection for the underlying bedrock aquifer, which is not taken into account by the DRASTIC index.

Comparing HVI and DRASTIC indices

The two vulnerability indices (Fig. 7 and Fig. 8) do not show the same spatial distribution because they do not integrate the same parameters. The HVI reflects a cumulative sequence of hydrochemical processes, from the recharge area to the aquifer domain where renewal rates are low. It can be considered as an integrated representation of the flow lines from the recharge area to the pumped well, and reflects borehole vulnerability. The DRASTIC index is mostly based on parameters responsible for vertical flows from the surface to the aquifer. It maps areas of potential groundwater contamination and does not consider flow line distribution or convergence of diffuse pollution to a well, nor does it take into account groundwater flow dynamics. For instance, an area covered with impermeable sediment will be associated with a low DRASTIC index, but groundwater at this site may be affected by contamination from neighbouring upstream vulnerable areas where recharge occurs.

Nitrate is highly leachable in groundwater and is often chosen to trace anthropogenic impacts on groundwater resource at regional scales (Rodriguez-Galiano 2014). It is also the contaminant that most frequently exceeds drinking water standard (e.g. MENV, 2004; U.S. Environmental Protection Agency, 2005; Stuart et al., 2007). However, because it is subject to denitrification, nitrate is not a perfect tracer. Previous studies detailed the processes involved for denitrification due to oxic/anoxic conditions (Korom, 1992, McMahon et al., 2003) which are associated to microbial (McMahon et al., 2008) or pyrite reduction (Böhlke et al, 2002) in groundwater. In the current study, denitrification rates were not estimated because of the density of sampling locations and because of the relatively low nitrate concentrations measured.

The HVI and DRASTIC indices were compared against measured nitrate concentrations to estimate the predicting capacity of the vulnerability method (note: the HVI computation does not include nitrate). The occurrence of nitrate in groundwater depends 1) on the spatial distribution of non-point sources of contamination at the land surface, 2) on the capacity of nitrogen to be mineralized and migrate vertically through the unsaturated zone towards the aquifer, and 3) on groundwater flow paths within the saturated zone. Directly comparing the HVI and DRASTIC vulnerability scores with the occurrence of nitrate therefore provides a means to evaluate how each

of these causes influences nitrate concentrations at a given well. To compare the two vulnerability indices with the nitrate and within a single range, DRASTIC indices (from 33 to 179) were linearized to values between 1 and 10 (Fig. 9). For samples with detected nitrate, the linearized DRASTIC index ranges between 4.5 and 8.7 but does not show a gradual increase pattern with nitrate concentrations. This result suggests that the DRASTIC index is relatively ineffective for evaluating more and less vulnerable areas in the study area. In sharp contrast, the HVI shows a consistent trend with the occurrence of nitrate within the Becancour area, with 82% of all wells having detectable nitrate concentrations (above 0.1 mg $N\text{-}NO_3$/L) having a vulnerability score of greater than 9.

Because both methods estimate the intrinsic vulnerability, neither considers the presence of a contaminant source at the surface and the difference between their capacities to identify the presence of nitrate in groundwater is linked to one of the other two causes. The better nitrate/vulnerability index correspondence for the HVI method is probably explained by the fact that major ions geochemistry reflects groundwater flow dynamics which are not considered in DRASTIC. The inclusion of parameters considered representative of contaminant migration through the unsaturated zone is not sufficient for DRASTIC to identify correctly nitrate concentrations. Using concentrations from other anthropogenic contaminants, performing tracer tests or groundwater flow modelling on the studied aquifer would provide a more complete test of the HVI method capacity to identify regional scale groundwater vulnerability.

Conclusions

The objective of this work was to test the potential of major ion chemistry to assess groundwater vulnerability of a regional aquifer. A Hydrogeochemical Vulnerability Index (HVI) was developed and applied to a southern Quebec fractured bedrock aquifer and results were compared to those of the classical DRASTIC method, and to measured nitrate concentrations.

Major ion of groundwater samples evolve from Ca,Mg-HCO_3 type in recharge areas to Na-HCO_3 and Na-Cl type downgradient in the aquifer. Although relatively low, nitrate concentrations in nearly 13% of the sampled wells show anthropogenic impacts from agricultural activities. The proposed HVI integrates processes from both infiltration and groundwater flow dynamics, and shows scores consistent with the occurrence of nitrate in groundwater. It also highlights local discontinuities in confinement that differ from the regional pattern. Eighty-two percent of all

groundwater samples with detectable nitrate groundwater show a HVI close to the maximum value of 10, a performance significantly better than that of the DRASTIC index. The poor correlation between the DRASTIC index and the nitrate concentration in groundwater is probably due to the fact that the DRASTIC method does not include groundwater flow dynamics.

This work shows that major ion geochemistry contains significant information about intrinsic well vulnerability. This inexpensive and easily implemented method is transferrable to similar geological contexts but would need to be adapted if carbonate dissolution and cation exchange are not the main hydrogeochemical processes which control the groundwater composition locally and regionally. It would also need to be tested using concentrations of other anthropogenic contaminants and confronted to other vulnerability methods. Combining the hydrogeochemical vulnerability method with the mapping of non-point sources of anthropogenic pollution at the land surface may contribute a real support tool for groundwater integrated resource-protecting policies.

Acknowledgments

We wish to thank an anonymous reviewer for his careful review and suggestions that greatly improved the manuscript. The authors thank the Quebec Ministry of Environment (*Ministère du Développement durable, de l'Environnement et de la Lutte contre les changements climatiques)*, the Becancour River Watershed organization (*organisme de bassin versant GROBEC*) and the municipalities that have participated in financing and supporting this research.

References

Aller L, Bennett T, Lehr JH, Petty RJ, Hackett G (1987) DRASTIC: A Standardized System for Evaluating Groundwater Pollution Potential Using Hydrogeologic Settings. EPA-600/2-87-035, 20 p.

Andrade AIASS, Stigter TY (2009) Multi-method assessment of nitrates and pesticides contamination in shallow alluvial groundwater as a function of hydrogeologic setting and land use. Agr Water Manage 96:1751–1765.

Appelo CAJ, Postma D (2005) Geochemistry, Groundwater and Pollution, 2nd ed. A.A. Balkema Publishers, Leiden, The Netherlands, 649 p.

Barbecot F, Marlin C,.Gibert E, Dever L (2000) Hydrochemical and isotopic characterisation of the Bathonian and Bajocian coastal aquifer of the Caen area (northern France). App Geochem 15, 6:791-805.

Beaudry C (2013) Hydrogéochimie de l'aquifère rocheux régional en Montérégie est, Québec. MSc thesis, INRS-ETE, Université du Québec, Québec, Canada, 210 p. Access to the geochemical dataset online : http://sdis.inrs.ca/ (in French)

Benoit N, Nastev M, Blanchette D, Molson J (2014) Hydrogeology and hydrogeochemistry of the Chaudière River watershed aquifers, Quebec, Canada. Can Water Resour J 39:1:32-48.

Bojórquez-Tapia A, Cruz-Bello GM, Luna-González L, Juárez L, Ortiz-Pérez MA (2009) V-DRASTIC: using visualization to engage policymakers in groundwater vulnerability assessment. J Hydrol 373: 242–255.

Böhlke, JK, Wanty, R, Tuttle, M, Delin, G, Landon, M (2002) Denitrification in the recharge area and discharge area of a transient agricultural nitrate plume in a glacial outwash sand aquifer, Minnesota. Water Resour. Res. 38:7, doi: 10.1029/2001WR000663.

Carrier MA, Lefebvre R, Rivard C, Parent M, Ballard JM, Benoit N, Vigneault H, Beaudry C, Malet X, Laurencelle M, Gosselin JS, Ladevèze P, Thériault R, Beaudin I, Michaud A, Pugin A, Morin R, Crow H, Gloaguen E,Bleser J, Martin A, Lavoie D (2013) Portrait des ressources en eau souterraine en Montérégie Est, Québec, Canada. Projet réalisé conjointement par l'INRS, la CGC, l'OBV Yamaska et l'IRDA dans le cadre du Programme d'acquisition de connaissances sur les eaux souterraines,rapport final INRS R-1433, soumis en juin 2013, 312p. (in French)

426 CEAEQ (Centre d'expertise en analyse environnementale du Québec) (2014) Les méthodes
427 d'analyses en usage au Centre d'expertise en analyse environnementale. On-line :http://
428 www.ceaeq.gouv.qc.ca/methodes/methode_index.htm
429 Champagne L (1990) Vulnérabilité des eaux souterraines à la pollution : M.R.C. de Montcalm. MSc
430 thesis, Université de Montréal, Québec, Canada, 80 p. (in French)
431 Charron JE (1978) Hydrogeochemical Study of Groundwater Flow in the Interstream Area between
432 the Ottawa and St. Lawrence Rivers. Environment Canada, Water Resource Branch, Scientific
433 series NO.76. 45 p.
434 Chen SK, Jang CS, Peng YP (2013) Developing a probability-based model of aquifer vulnerability
435 in an agricultural region. J Hydrol 486:494–504.
436 Chowdhury SH, Kehew AE, Passero RN (2003) Correlation between nitrates contamination and
437 groundwater pollution potential. Groundwater 41:735-745.
438 Cloutier V, Lefebvre R, Therrien R, Savard MM (2008) Multivariate statistical analysis of
439 geochemical data as indicative of the hydrogeochemical evolution of groundwater in a
440 sedimentary rock aquifer system. J Hydrol 353:294-313.
441 Cloutier V, Lefebvre R, Therrien R, Savard MM (2010) Desalination of a sedimentary rock aquifer
442 system invaded by Pleistocene Champlain Sea water and processes controlling groundwater
443 geochemistry. Environ Earth Sci 59:977-994.
444 Dubrovsky NM, Burow KR, Clark GM, Gronberg JM, Hamilton PA, Hitt KJ, Mueller DK, Munn
445 MD, Nolan BT, Puckett LJ, Rupert MG, Short TM, Spahr NE, Sprague LA, Wilber WG (2010)
446 The quality of our Nation's waters—Nutrients in the Nation's streams and groundwater, 1992–
447 2004. U.S. Geological Survey Circular 1350, 174 p.
448 Edmunds WM, Shand P, Hart P, Ward RS (2003) The natural (baseline) quality of groundwater: a
449 UK pilot study. The Sci Total Environ 310:25-35.
450 Edmunds WM, Cook JM, Darling WG, Kinniburgh DG, Miles DL, Bath AH, Morganjones M,
451 Andrews JN (1987) Baseline geochemical conditions in the Chalk aquifer, Berkshire, U.K: a
452 basis for groundwater quality management. App Geochem, 2:251-274.
453 Environment Canada (2012) Canadian climate normals 1971-2000 for Laurierville, Québec. On-
454 line:http://climate.weather.gc.ca/climate_normals/index_e.html
455 EPA (Environmental Protection Agency) (1993) A review of methods for assessing aquifer
456 sensitivity and groundwater vulnerability to pesticide contamination. EPA-813-R-93002, 147 p.

457 Frind EO, Molson JW, Rudolph DL (2006) Well Vulnerability: A Quantitative Approach for
458 Source Water Protection. Groundwater 44:732-742.
459 Globensky Y (1987) Géologie des Basses-Terres du Saint-Laurent, Québec. Ministère des
460 Richesses Naturelles du Québec 63 (v. MM 85-02). (in French).
461 Globensky Y (1993) Lexique stratigraphique canadien. Volume V-B: région des Appalaches, des
462 Basses-Terres du Saint-Laurent et des Iles de la Madeleine. Ministère de l'Énergie et des
463 Ressources et Direction Générale de l'Exploration géologique et minérale, p. 327, DV 91e23.
464 (in French).
465 Godbout PM, Lamothe M, Horoi V, Caron O (2011) Synthèse stratigraphique, cartographie des
466 dépôts quaternaires et modèle hydrostratigraphique régional, secteur de Bécancour, Québec:
467 Rapport final. Report presented to the Ministère des Ressources naturelles, 37 p. (in French).
468 IRDA (Institut de recherche et de développement en agroenvironnement) (2012) Feuillets
469 pédologiques numériques 1 : 20 000: 21L12, 21L06, 21L05, 21L04, 21L03, 31I09, 31I08,
470 31I07, 31I02, 31I01.
471 Korom, SF (1992) Natural denitrification in the saturated zone: a review.Water Resour. Res., 28,
472 1657– 1668.
473 Kozuskanich JC, Novakowski KS, Anderson BC, Crowe AS, Balakrishnan YK (2014)
474 Anthropogenic Impacts on a Bedrock Aquifer at the Village Scale. Groundwater 52:474–486.
475 Lamothe M (1989) A new framework for the Pleistocene stratigraphy of the central St. Lawrence
476 Lowland, southern Quebec. Géographie Physique et Quarternaire 43:119-129.
477 Larocque M, Gagné S, Barnetche D, Meyzonnat G, Graveline MH, Ouellet MA (2015) Projet de
478 connaissance des eaux souterraines du bassin versant de la zone Nicolet et de la partie basse de
479 la zone Saint-François. Rapport scientifique. Report submitted to the Ministère du
480 Développement durable, de l'Environnement et de la Lutte contre les changements climatiques.
481 260 p. (in French)
482 Larocque M, Gagné S, Tremblay L, Meyzonnat G (2013) Projet de connaissance des eaux
483 souterraines du bassin versant de la rivière Becancour et de la MRC de Becancour - Rapport
484 scientifique. Report submitted to the Ministère du Développement durable, de l'Environnement,
485 de la Faune et des Parcs, 213 p. (in French).
486 McMahon, PB, Böhlke, JK, Kauffman, LJ, Kipp, KL, Landon, MK, Crandall, CA, Burow, KR,
487 Brown, CJ (2008) Source and transport controls on the movement of nitrate to public supply

488 wells in selected principal aquifers of the United States, Water Resour. Res. 44, W04401,
489 doi:10.1029/2007WR006252.
490 McMahon, PB, Böhlke, Christenson, SC (2004) Geochemistry, radiocarbon ages, and
491 paleorecharge conditions along a transect in the central High Plains aquifer, southwestern
492 Kansas, USA. App Geochem, 19:1655-1686.
493 Mansoor A, Baloch MA, Sahar L (2014) Development of a Watershed-Based Geospatial
494 Groundwater Specific Vulnerability Assessment Tool. Groundwater 52:137-147.
495 MDDEFP (Ministère du Développement durable, de l'Environnement, de la Faune et des Parcs).
496 (2013) Règlement sur la qualité de l'eau potable. c. Q-2, r. 40.
497 http://www2.publicationsduquebec.gouv.qc.ca/ (in French).
498 Mendizabal I, Stuyfzand PJ (2011) Quantifying the vulnerability of well fields towards
499 anthropogenic pollution: The Netherlands as an example. J Hydrol 398:260-276.
500 Mehnert E, Keefer DA, Dey WS, Wehrmann HA, Wilson SD, Ray C (2005) Aquifer sensitivity to
501 pesticide leaching: testing a soil and hydrogeologic index method. Groundwater Monitoring &
502 Remediation 25:60–67.
503 MENV (Ministère de l'Environnement) (2004) Étude de la qualité de l'eau potable dans sept
504 bassins versants en surplus de fumier et impacts potentiels sur la santé. Ministère de
505 l'Environnement du Québec, Québec, Canada, Envirodoq ENV/2004/0312. 137p. (in French).
506 MRNF (Ministère des Ressources naturelles et de la Faune) (2008) Digital elevation model
507 1:20 000, 21L12, 21L06, 21L05, 21L04, 21L03, 31I09, 31I08, 31I07, 31I02, 31I01. Ministère
508 des Ressources naturelles et de la Faune.
509 Murat V (2000) Étude comparative des méthodes d'évaluation de la vulnérabilité intrinsèque des
510 aquifères à la pollution: application aux aquifères granulaires du piémont Laurentien. MSc
511 thesis, INRS-ETE, Université du Québec, Québec, Canada, 291 p. (in French).
512 Nobre RCM, Filho OCR, Mansur WJ, Consenza CAN (2007) Groundwater vulnerability and risk
513 mapping using GIS modeling and and a fuzzy logic tool. J Contam Hydrol 94:277-292.
514 Qi Z, Helmers MJ, Christianson RD, Pederson CH (2011) Nitrate-nitrogen losses through
515 subsurface drainage under various agricultural land covers. J Environ Qual 40:1578-85.
516 Rodriguez-Galiano V, Mendes MP, Garcia-Soldado MJ, Chica-Olmo M, Ribeiro L (2014)
517 Predictive modeling of groundwater nitrate pollution using Random Forest and multisource

variables related to intrinsic and specific vulnerability: A case study in an agricultural setting (Southern Spain). Sci Total Environ 476–477, 189–206.

Rupert, MG (2001) Calibration of the DRASTIC groundwater vulnerability mapping method. Groundwater 39:625-630.

Saeedi M, Abessi O, Sharifi F, Meraji H (2009) Development of groundwater quality index. Environ Monit Assess 163, 327-335.

Saidi S, Bouri S, Ben Dhia H (2010) Groundwater vulnerability and risk mapping of the Hajeb-jelma aquifer (Central Tunisia) using a GIS-based DRASTIC model. Environ Earth Sci 59:1579–1588

Sorichetta A, Ballabio C, Masetti M, Robinson GR, Sterlacchini S (2013) A Comparison of Data-Driven Groundwater Vulnerability Assessment Methods. Groundwater 51: 866–879.

Stigter TY, Ribeiro L, Carvalho Dill AMM (2008) Building factorial regression models to explain and predict nitrates concentrations in groundwater under agricultural land. J Hydrol 357:42-56.

Stuart ME, Chilton PJ, Kinniburgh DG, Cooper DM (2007) Screening for long-term trends in groundwater nitrate monitoring data. Quarterly Journal of Engineering Geology and Hydrogeology 40:361–376.

Tilahun K, Merket BJ (2010) Assessment of groundwater vulnerability to pollution in Dire Dawa, Ethiopia using DRASTIC. Environ Earth Sci 59:1485–1496

United Nations Environment Programme (2003) Groundwater and its susceptibility to degradation: A global assessment of the problem and options for management, ISBN: 92-807-2297-2. 140 p.

U.S. Environmental Protection Agency (2005) Factoids: Drinking Water and Ground Water Statistics for 2004, EPA 816-K-05-001, 15 p.

Van Stempvoort D, Ewert L, Wassenaar L (1992) AVI: A Method for Groundwater Protection Mapping in the Prairie. Provinces of Canada. Prairie Provinces Water Board Report No. 114.

Vrba J, Zoporozec A (1994) Guidebook on Mapping Groundwater Vulnerability. IAH International Contribution for Hydrogegology, Hannover, Germany, 160 p.

Yu C, Yao Y, Cao, G, Zheng, C (2014) A field demonstration of groundwater vulnerability assessment using transport modeling and groundwater age modeling, Beijing Plain, China. Environ Earth Sci DOI 10.1007/s12665-014-3769-5

Zhou J, Li Q, Guo Y, Guo X, Li X, Zhao Y, Jia R (2012) VLDA model and its application in assessing phreatic groundwater vulnerability: a case study of phreatic groundwater in the plain area of Yanji County, Xinjiang, China. Environ Earth Sci 67:1789–1799

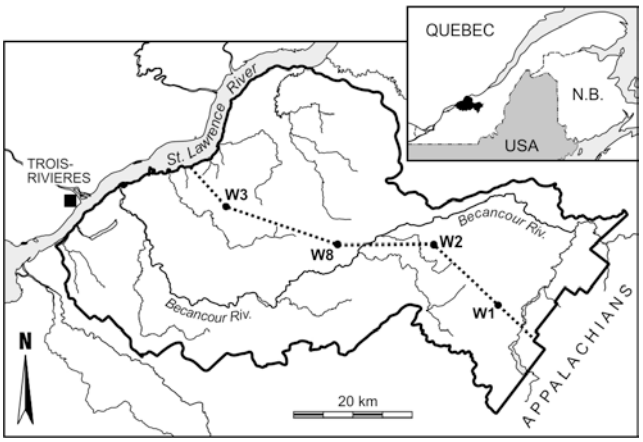

Fig. 1. The Becancour watershed with location of the cross section of Fig. 2.

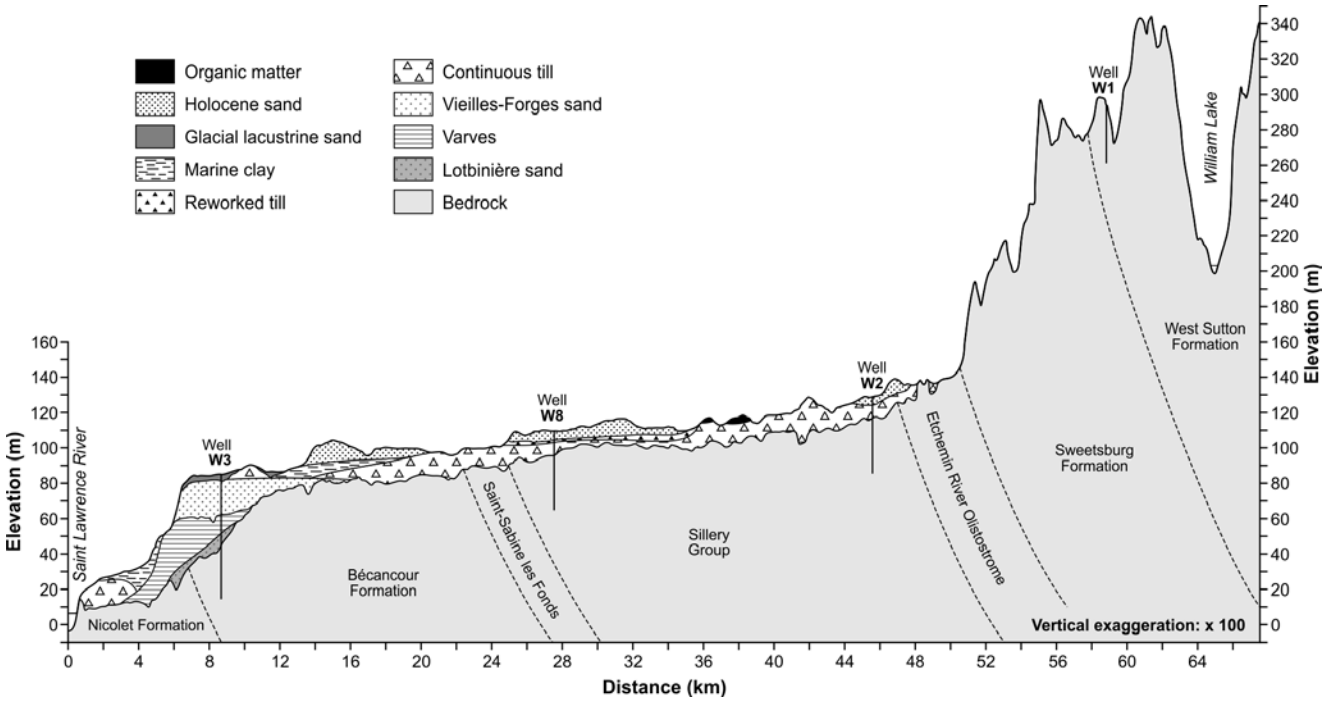

Fig. 2. SE-NW geological cross section of the Becancour watershed.

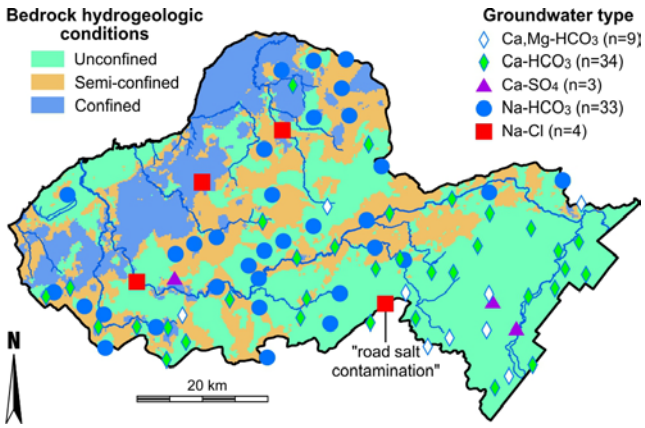

Fig. 3. Groundwater types and bedrock aquifer confinement conditions.

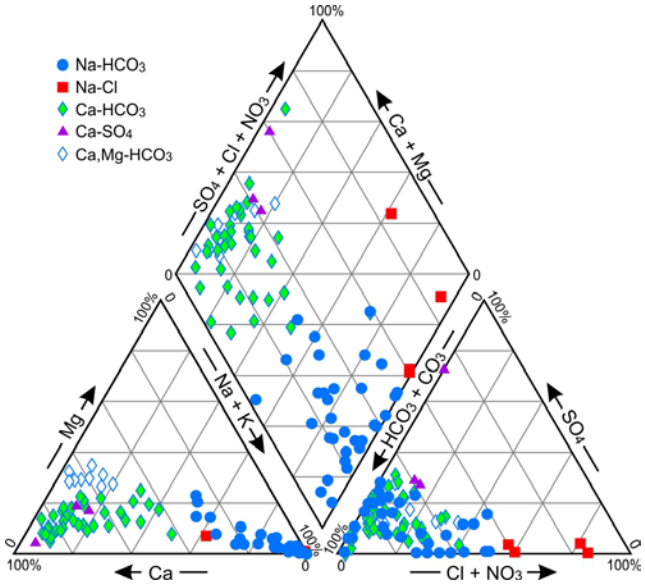

Fig. 4. Piper tri-linear plot of groundwater samples.

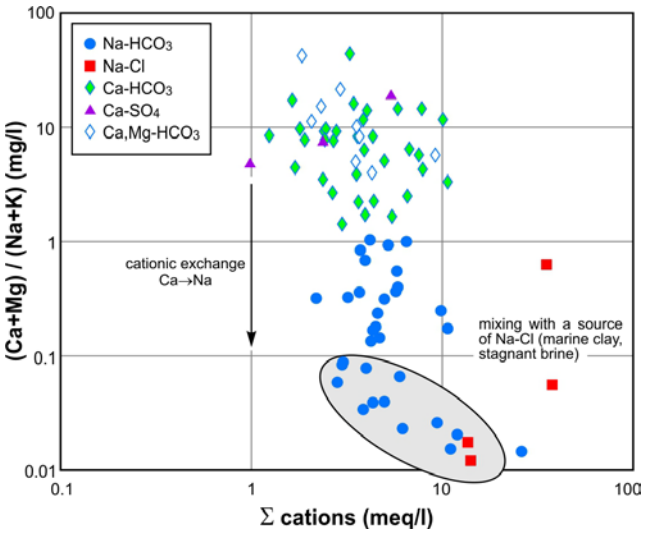

562

563 **Fig. 5**. Cationic exchange evidence in groundwater.

564

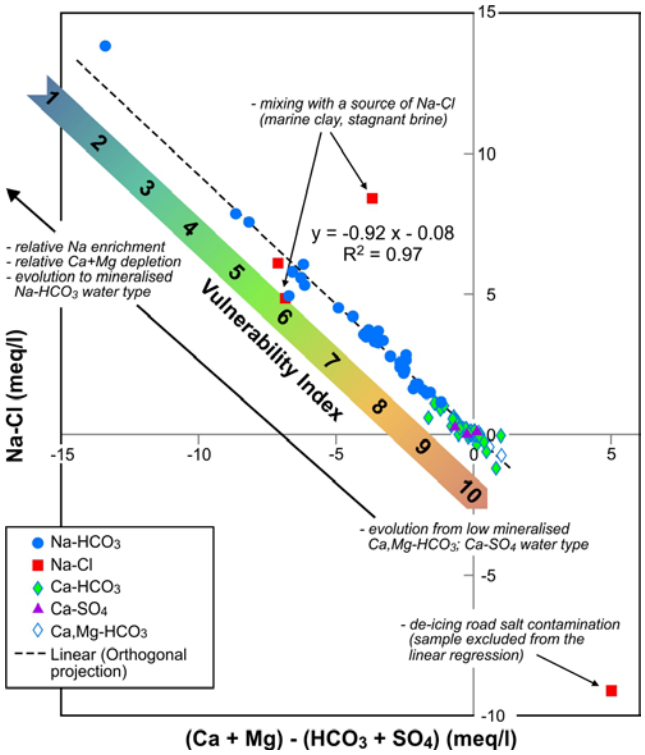

565

566 **Fig. 6**. The Hydrogeochemical Vulnerability Index (HVI).

567

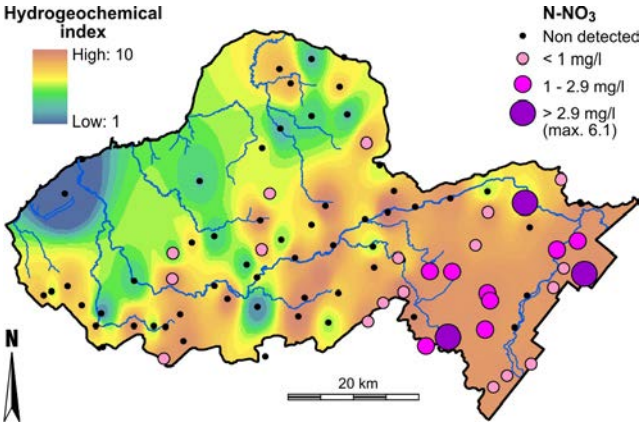

Fig. 7. Vulnerability map obtained using the Hydrogeochemical Vulnerability Index (HVI).

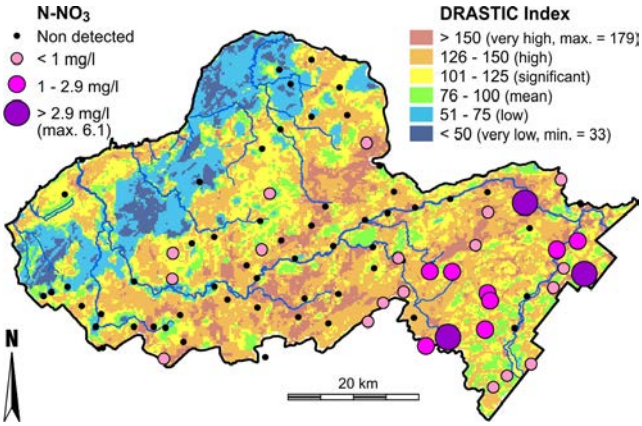

Fig. 8. Vulnerability map obtained using the DRASTIC index (DI).

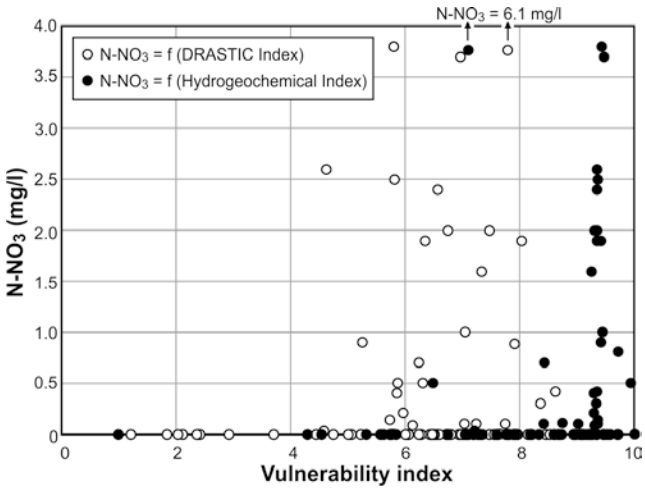

Fig. 9. Comparison of vulnerability maps with measured nitrate concentrations.

579

580 **Table 1**. Hydrogeochemical data

Sample name	Total well depth (m)	Ca (mg/L)	Mg (mg/L)	K (mg/L)	Na (mg/L)	HCO_3 (mg/L)	Cl (mg/L)	SO_4 (mg/L)	$N\text{-}NO_3$ (mg/L)
BEC001	51.8	5.9	0.9	0.4	130.0	316,8	13.0	63.0	0.0
BEC002	17.1	94.0	21.0	3.4	31.0	353,7	52.0	40.0	0.0
BEC003	22.9	72.0	6.8	3.6	16.0	219,5	37.0	21.0	0.0
BEC005	18.3	3.5	0.7	4.1	210.0	414,7	47.0	100.0	0.0
BEC007	44.0	8.4	3.1	2.0	87.0	241,7	19.0	15.0	0.0
BEC008	17.0	2.2	0.7	1.5	320.0	411,5	280.0	24.0	0.0
BEC009	50.3	32.0	3.1	2.9	9.9	146,3	1.8	0.0	0.0
BEC010	37.0	32.0	6.6	2.0	4.9	121,9	0.9	24.0	0.0
BEC011	22.0	13.0	1.7	2.0	55.0	182,7	0.7	23.0	0.0
BEC012	32.6	58.0	7.7	2.7	5.1	158,5	52.0	6.3	0.0
BEC014	41.1	2.2	0.7	1.3	250.0	389,9	190.0	3.1	0.0
BEC015	33.5	3.0	1.0	1.5	63.0	181,6	0.6	14.0	0.0
BEC016	26.0	15.0	2.6	2.7	61.0	182,7	32.0	0.0	0.0
BEC021	25.9	45.0	14.0	2.4	18.0	146,2	46.0	22.0	0.0
BEC022	45.7	3.0	0.5	1.4	110.0	230,6	48.0	0.5	0.0
BEC024	27.4	2.6	0.4	1.0	96.0	230,6	0.8	37.0	0.0
BEC026	10.7	130.0	21.0	5.7	51.0	451,3	79.0	28.0	0.0
BEC027	21.0	20.0	2.2	2.0	86.0	231,6	16.0	33.0	0.0
BEC028	30.5	26.0	2.6	3.3	95.0	170,7	85.0	41.0	0.0
BEC029	27.4	57.0	6.2	3.7	9.6	146,3	37.0	24.0	0.0
BEC030	27.7	2.3	0.1	2.9	85.0	182,6	0.7	46.0	0.0
BEC031	18.3	23.0	6.7	6.4	43.0	195,1	12.0	17.0	0.0
BEC032	21.0	130.0	9.9	3.9	8.8	402,5	14.0	26.0	1.0
BEC033	49.4	7.9	1.2	3.8	84.0	206,9	2.4	44.0	0.0
BEC034	24.4	27.0	3.9	1.9	16.0	121,9	2.7	18.0	0.0
BEC035	38.1	9.7	1.3	2.4	94.0	158,1	64.0	25.0	0.0
BEC036	58.5	100.0	34.0	1.6	30.0	353,7	75.0	48.0	0.5
BEC040	14.5	19.0	1.9	1.0	2.3	47,57	3.6	12.0	2.6
BEC041	61.0	55.0	5.4	0.4	1.4	158,5	2.3	24.0	0.9
BEC042	80.8	41.0	1.4	0.4	5.0	120,7	7.2	8.0	0.1
BEC043	44.2	2.5	1.3	2.3	310.0	426,7	310.0	3.4	0.0
BEC044	84.2	97.0	2.9	0.3	5.8	121,9	0.7	180.0	0.0
BEC045	70.1	69.0	3.9	0.9	5.4	207,3	5.7	27.0	0.4
BEC046	68.6	40.0	15.0	0.8	6.8	158,5	18.0	26.0	0.0
BEC050	38.1	40.0	11.0	3.8	11.0	158,5	6.4	42.0	0.0
BEC052	88.4	14.0	2.1	2.4	85.0	243,9	5.8	43.0	0.0
BEC053	39.0	88.0	17.0	3.3	18.0	341,5	18.0	48.0	0.0
BEC055	18.3	54.0	6.3	1.3	7.7	158,5	13.0	34.0	0.0
BEC056	100.6	24.0	9.1	3.2	180.0	353,7	120.0	51.0	0.5
BEC057	20.7	32.0	5.4	2.4	85.0	268,3	55.0	9.9	0.0
BEC100	51.8	8.9	1.0	0.8	38.0	105,0	7.6	20.0	0.7
BEC101	47.2	1.2	0.3	1.1	210.0	413,8	150.0	2.2	0.0
BEC102	21.6	55.0	8.3	2.4	44.0	268,3	37.0	12.0	0.0
BEC103	43.6	73.0	13.0	3.1	40.0	268,3	62.0	41.0	0.0
BEC104	28.0	24.0	2.3	1.0	6.3	76,82	11.0	8.6	0.4
BEC107	36.6	33.0	5.4	0.8	5.8	101,1	9.6	32.0	0.1
BEC110	37.8	43.0	11.0	1.8	29.0	195,1	5.8	60.0	0.0
BEC112	38.1	32.0	11.0	2.0	24.0	207,3	1.7	8.1	0.1
BEC115	68.6	24.0	7.2	0.3	0.8	98,81	0.4	7.6	0.1

BEC116	45.7	26.0	7.2	1.2	3.1	98,81	4.8	9.3	2.4
BEC119	45.7	21.0	6.9	2.6	53.0	170,7	43.0	0.0	0.0
BEC120	68.6	21.0	7.5	2.2	96.0	292,6	34.0	17.0	0.0
BEC121	99.1	3.3	0.9	1.8	270.0	512,2	150.0	0.0	0.0
BEC122	38.1	29.0	13.0	4.4	60.0	317,1	3.3	1.0	0.0
BEC123	54.9	45.0	3.1	1.1	5.3	115,8	5.3	32.0	0.3
BEC126	49.1	25.0	6.2	0.9	27.0	134,1	26.0	7.6	0.0
BEC127	25.9	30.0	1.4	0.4	3.4	79,29	5.4	11.0	1.9
BEC129	61.0	36.0	4.0	1.5	47.0	207,3	23.0	22.0	0.1
BEC130	91.4	150.0	22.0	2.4	16.0	426,9	34.0	93.0	0.0
BEC131	22.9	30.0	8.0	0.4	3.0	117,1	2.2	9.7	2.0
BEC132	38.1	39.0	10.0	1.4	2.1	134,1	3.0	20.0	3.8
BEC134	38.1	97.0	7.0	2.8	6.6	256,1	6.1	63.0	2.0
BEC135	44.2	54.0	6.1	1.0	3.8	170,7	1.9	18.0	1.9
BEC137	23.7	5.1	0.4	1.6	85.0	219,5	9.4	29.0	0.0
BEC138	32.0	42.0	3.3	1.4	6.0	158,5	2.7	2.4	0.0
BEC139	48.8	0.1	0.0	0.1	88.0	95,13	11.0	100.0	6.1
BEC140	33.5	28.0	1.6	1.6	1.0	100,0	0.2	5.0	0.2
BEC142	68.6	44.0	13.0	1.2	8.3	195,1	8.0	16.0	1.6
BEC143	51.2	30.0	2.1	0.4	4.5	108,5	0.5	19.0	0.0
BEC144	8.2	100.0	17.0	6.2	21.0	439,1	11.0	40.0	0.0
BEC145	13.7	35.0	18.0	8.0	71.0	304,9	53.0	22.0	0.0
BEC146	30.5	35.0	9.3	2.3	31.0	219,5	9.0	17.0	0.0
BEC149	54.9	50.0	4.0	2.0	15.0	195,1	5.7	14.0	0.1
BEC160	144.8	41.0	2.1	1.0	4.5	113,4	9.5	7.4	3.7
BEC161	8.5	33.0	3.5	1.6	15.0	146,3	4.1	14.0	0.0
BEC165	106.7	220.0	31.0	3.5	500.0	426,9	1100.0	74.0	0.9
BEC166	73.2	20.0	6.9	3.9	210.0	451,0	120.0	36.0	0.0
ROC01	30.0	13.0	2.0	0.6	3.4	31,71	2.2	9.5	2.5
ROC03	78.3	24.0	9.4	6.8	820.0	340,9	970.0	3.0	0.0
ROC04	36.6	6.8	3.3	0.8	85.0	206,5	2.4	33.0	0.0
ROC05	47.2	1.9	0.5	1.6	140.0	365,2	3.0	16.0	0.0
ROC06	42.7	1.6	0.9	2.3	60.0	133,0	0.7	22.0	0.0
ROC08	43.5	3.8	0.6	0.8	64.0	157,9	0.5	6.6	0.0
ROC09	35.7	3.1	2.6	3.4	590.0	828,8	420.0	7.5	0.0

581